JMEPEG (2010) 19:129–134
DOI: 10.1007/s11665-009-9423-9

1059-9495/$19.00

Growth Behavior of Intermetallic Compounds at SnAgCu/Ni and Cu Interfaces

Lihua Qi, Jihua Huang, Hua Zhang, Xingke Zhao, Haitao Wang, and Donghai Cheng

(Submitted March 20, 2008; in revised form February 26, 2009)

The growth behavior of reaction-formed intermetallic compounds (IMCs) at Sn3.5Ag0.5Cu/Ni and Cu interfaces under thermal-shear cycling conditions was investigated. The results show that the morphology of $(Cu_xNi_{1-x})_6Sn_5$ and Cu_6Sn_5 IMCs formed both at Sn3.5Ag0.5Cu/Ni and Cu interfaces gradually changed from scallop-like to chunk-like, and different IMC thicknesses developed with increasing thermal-shear cycling time. Furthermore, Cu_6Sn_5 IMC growth rate at the Sn3.5Ag0.5Cu/Cu interface was higher than that of $(Cu_xNi_{1-x})_6Sn_5$ IMC under thermal-shear cycling. Compared to isothermal aging, thermal-shear cycling led to only one Cu_6Sn_5 layer at the interface between SnAgCu solder and Cu substrate after 720 cycles. Moreover, Ag_3Sn IMC was dispersed uniformly in the solder after reflow. The planar Ag_3Sn formed near the interface changed remarkably and merged together to large platelets with increasing cycles. The mechanism of formation of Cu_6Sn_5, $(Cu_xNi_{1-x})_6Sn_5$ and Ag_3Sn IMCs during thermal-shear cycling process was investigated.

Keywords Ag_3Sn, growth behavior, intermetallic compound (IMC), Sn3.5Ag0.5Cu solder, thermal-shear cycling

1. Introduction

The Sn-Pb eutectic solder is one of the best solders due to its wettability and low melting point. But Pb is prohibited in the electronic production because of its deleterious effect on the environment and human health. In order to replace the Pb in Sn-Pb solder, SnAgCu solders were considered as promising because their microstructure is denser and IMC growth rate is lower than that of Sn-Zn, Sn-Cu, and Sn-Ag systems (Ref 1-4). At present, microstructure transformation in IMCs and growth behavior at both SnAgCu/Cu and SnAgCu/Ni interfaces have been researched for different reflow temperatures and isothermal aging times (Ref 1, 5, 6). It has been shown that IMC thickness formed at the two interfaces increases with isothermal aging (Ref 7, 8). In fact, the solder joints will experience the thermal and shear stress-strain cycling in service due to high cyclic stress generated by the mismatch of the coefficients of thermal expansion (CTE) between printed circuit board (PCB) and chip. Furthermore, because of low-melting point and low-recrystallization temperature of Sn-base solder, the stress-strain behavior has an effect on IMC growth at the interface. However, there has been little research on growth behavior of IMCs under thermal-shear cycling conditions. Specifically, the present paper has investigated the IMC growth behavior and formation mechanism at both Sn3.5Ag0.5Cu/Cu and Ni interfaces under thermal-shear cycling at 25-125 °C and isothermal aging at 125 °C conditions.

Lihua Qi, Jihua Huang, Hua Zhang, Xingke Zhao, Haitao Wang, and **Donghai Cheng**, School of Materials Science and Engineering, University of Science and Technology Beijing, 30# Xueyuan R.d., Haidian District, Beijing, P.R. China. Contact e-mail: qlh1973@163.com.

2. Experimental

A special specimen was designed to study the interfacial microstructure and the IMC growth in solder joints during thermal-shear cycling. The chip was taken to be a tungsten bar because of a similar thermal expansion coefficient (4.6×10^{-6}/°C), and copper bar replaced the PCB. Due to the poor wettability of SnAgCu solder on tungsten, nickel foils were selected to joint the two ends of tungsten through BNi2 brazing alloy, and has good weldability with SnAgCu solder. On the other hand, copper and tungsten bars are rigid bodies, and the low melting solder SnAgCu is a viscoelastic material (Ref 9). The deformation caused by copper and tungsten bars was mainly absorbed by the SnAgCu solder during experimental process. In the sample, a tungsten bar was first brazed with the nickel foils at both ends with BNi2 brazing alloy at 1120 °C for 20 min under a vacuum of 1.6×10^{-4} Pa and then soldered with a copper bar using Sn3.5Ag0.5Cu eutectic alloy, as shown in Fig. 1. The experimental process is as follows: the samples were put into the TSA-71S-A cold & hot blow test box, heated up from 25 to 125 °C in 5 min and preserved for 25 min at 125 °C, and then cooled down from 125 to 25 °C in 5 min and preserved for 25 min at 25 °C. This represented a cycle. The samples were subjected to 24, 200, 400 and 720 cycles, respectively. The solder joints at both ends of the samples will experience the thermal-shear cycling during the experiment due to CTE mismatch between copper and tungsten bars. The strain rate of the solder joints is 9.93×10^{-4}/s. The samples for isothermal aging test were put into a constant temperature box at 125 °C for 12, 100, 200, 360, and 720 h, respectively. The test specimens were prepared by cutting into small pieces ($5 \times 5 \times 2$ mm). The specimens were first cold mounted in

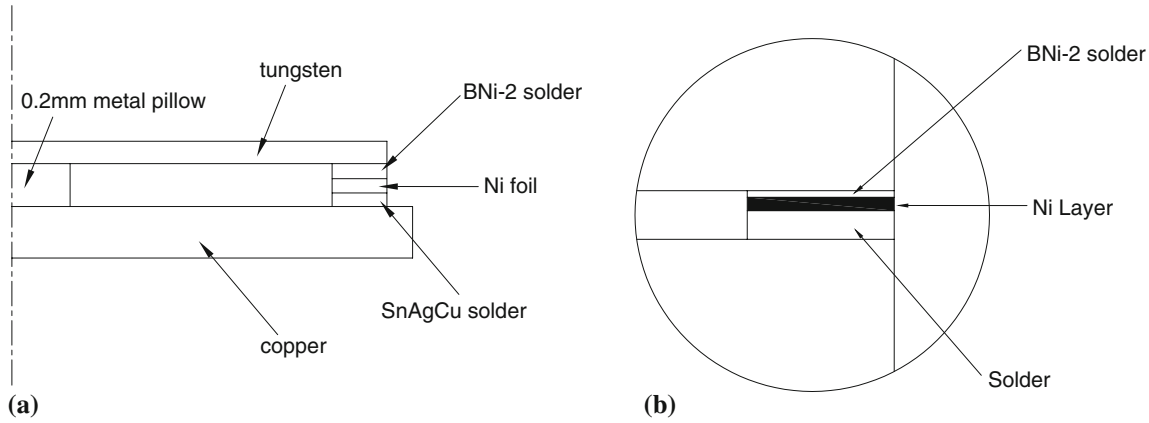

Fig. 1 Schematic of thermal-shear cycling test: (a) half-sample and (b) amplificatory picture of joint

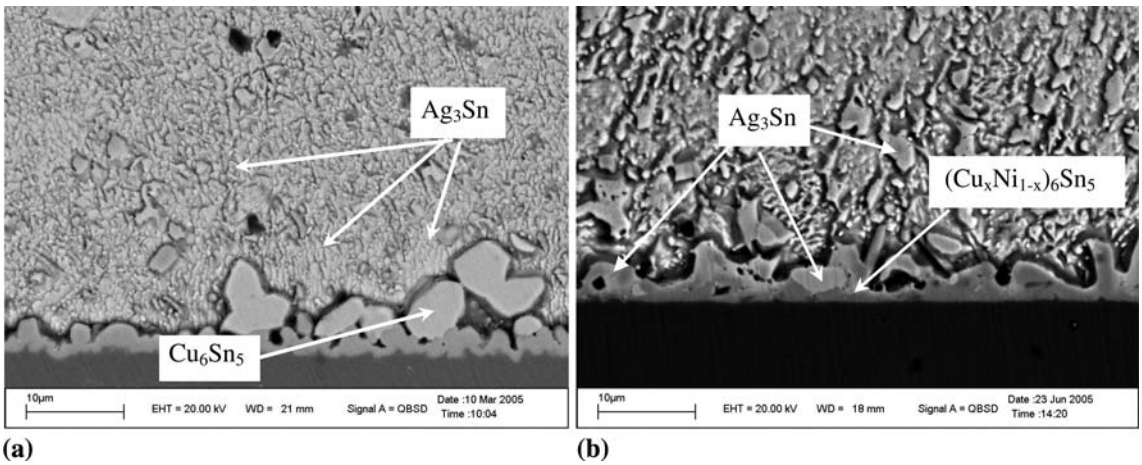

Fig. 2 SEM pictures of IMCs after thermal-shear cycling 24 cycles at (a) Sn3.5Ag0.5Cu/Cu and (b) Sn3.5Ag0.5Cu/Ni interface

epoxy, and then polished and etched with 5% HCl + 95% H_2O for observation of their microstructure and IMC growth behavior by scanning electron microscopy (SEM) and energy dispersion spectroscopy (EDS) and x-ray diffraction (XRD).

3. Results and Discussion

3.1 Intermetallic Morphology

Figure 2 presents the cross-section SEM image and EDS analyses at both the Sn3.5Ag0.5Cu/Cu and Sn3.5Ag0.5Cu/Ni interfaces after the thermal-shear cycling 24 times. At the Sn3.5Ag0.5Cu/Cu interface, a continuous and smooth scallop-like IMC layer is formed, the thickness of which is about 2.3 μm. At the Sn3.5Ag0.5Cu/Ni interface, a coarse and scattered IMC layer forms to an average thickness of 2.1 μm. The maximum thickness is about 4.5 μm, but the minimum film is only 0.5 μm. According to the EDS analysis, the components of IMC for Cu substrate are Cu 53.43 at.%, Sn 46.57 at.%, is Cu_6Sn_5. Similarly, the IMC for Ni substrate is $(Cu_xNi_{1-x})_6Sn_5$, Cu 42.54 at.%, Ni 15.76 at.% and Sn 41.70 at.%, based on Cu_6Sn_5. Therefore, Ni atoms can take the place of Cu atoms to form $(Cu_xNi_{1-x})_6Sn_5$ IMC because of the same crystal structure and nearly similar atomic numbers of Ni and Cu. Furthermore, Cu in $(Cu_xNi_{1-x})_6Sn_5$ IMC originates in the solder and Cu substrate, which illustrates that Cu atoms at the substrate can diffuse through the solder to the Ni substrate and react with Sn during the reflow process. Due to the difference of diffusion channel and distance of every Cu atom, the distribution morphology of IMC at the Ni substrate is uneven and scattered in liquid state. The total average thickness of $(Cu_xNi_{1-x})_6Sn_5$ at Ni substrate is less than that of Cu_6Sn_5 at Cu substrate. It is proved the Ni is more difficult to react with Sn base solder than Cu.

With the cycle times increasing, IMC morphology at Cu substrate changed gradually from scallop-like to planar-like and IMC thickness increased significantly. For the Ni substrate, a continuous $(Cu_xNi_{1-x})_6Sn_5$ IMC layer formed after 200 cycles due to dissolution and diffusion of Ni in the valley of two scallops. In solid state, atomic diffusion is very slow, for example, about 10^{-6} $\mu m^2/s$ at 125 °C and about 10^{-4} $\mu m^2/s$ at 180 °C (Ref 10, 11). Hence, the diffusion distance of Cu and Ni atoms from the valley of every two scallop-like phase to solder is short and IMC thickness grows remarkably, as shown in Fig. 3.

After 720 thermal-shear cycles, there is only one layer of Cu_6Sn_5 compound at the Cu substrate, and the thickness of planar-like Cu_6Sn_5 IMC is about 4.97 μm, as shown in Fig. 4(a). Therefore, the crystal lattice distortion generated by co-functions of thermal cycling and shear stress promotes Cu atom diffusion and Cu_6Sn_5 IMC growth. The Cu atoms of Cu_6Sn_5 IMC are provided mainly by the Cu substrate and less

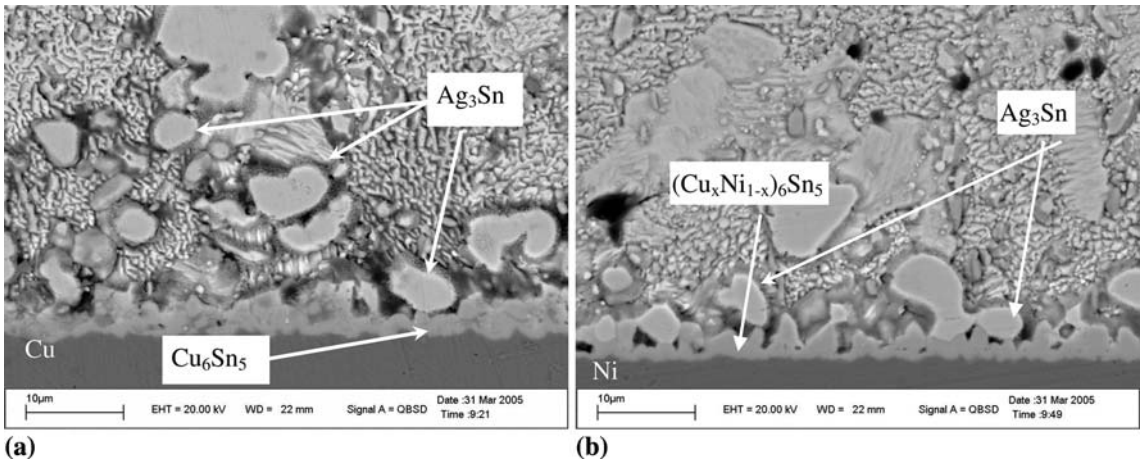

Fig. 3 SEM pictures after thermal-shear cycling 200 cycles at (a) Sn3.5Ag0.5Cu/Cu and (b) Sn3.5Ag0.5Cu/Ni interface

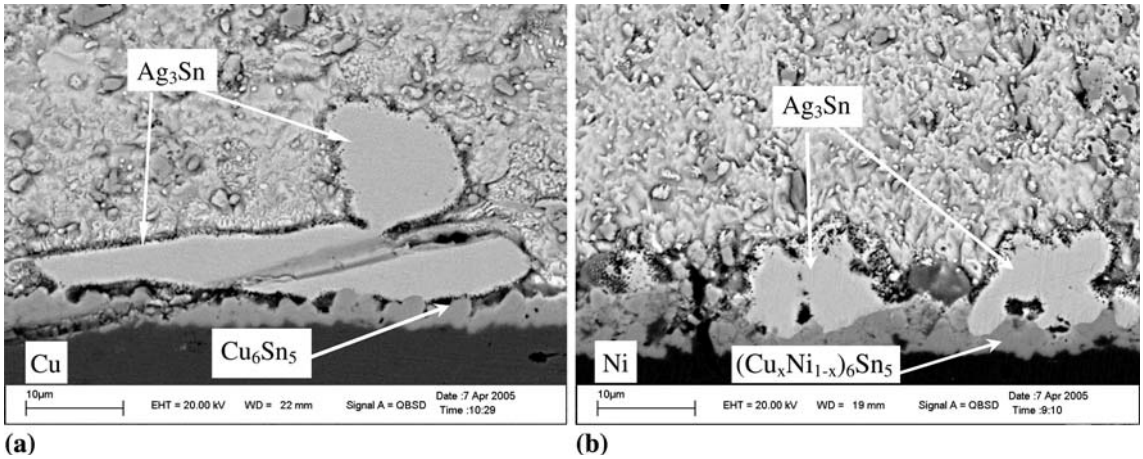

Fig. 4 SEM picture of IMCs after thermal-shear cycling 720 cycles at (a) Sn3.5Ag0.5Cu/Cu and (b) Sn3.5Ag0.5Cu/Ni interfaces

by the solder. For Sn3.5Ag0.5Cu/Ni interface, in Fig. 4(b), the average thickness of $(Cu_xNi_{1-x})_6Sn_5$ IMC develops slightly and the IMC morphology hardly changes. Therefore, Ni-electroplate layer is applied to restrain the IMC growth on the PCB because the diffusion rate of Ni is lower than that of Cu. However, the scallop-like $(Cu_xNi_{1-x})_6Sn_5$ IMC causes microcracks first under the bottom of scallop-type IMC, which then expand rapidly with an increase in the shear-strain such cracks are harmful to the stability of solder joints.

3.2 Intermetallic Growth Behavior

Intermetallic layer growth behavior at the SnAgCu/Cu and SnAgCu/Ni interfaces can be described by one-dimensional growth parameter, *Y*, which is related to the square root of the cycle time (Ref 12):

$$Y = Y_0 + (Dt)^{\frac{1}{2}} \quad \text{(Eq 1)}$$

$$D = D_0 \exp\left(-\frac{Q}{RT}\right) \quad \text{(Eq 2)}$$

where D is the diffusion coefficient given by an Arrhenius expression, Y_0 is the IMC thickness after reflow process, D_0 is the diffusion constant, Q the activation energy, R the Boltzmann constant, and T is the absolute temperature.

The measured intermetallic growth data at SnAgCu/Cu and SnAgCu/Ni interfaces after thermal-shear cycling and isothermal aging at 125 °C are given in Fig. 5. The IMC growth behavior can be fitted to *Y*, which is related to the square root of the thermal cycle time. Compared with the aging results, the IMC growth rate under thermal-shear cycling is larger than that under isothermal aging. On the one hand, thermal effect promotes atomic diffusion and IMC growth, and this is also identified by Pang (Ref 13); on the other hand, the shear stress-strain further accelerates atomic diffusion resulting in crystal lattice distortion. According to Fig. 5, the growth rate of Cu_6Sn_5 compound at the SnAgCu/Cu interface is larger than that of $(Cu_xNi_{1-x})_6Sn_5$ compound at the SnAgCu/Ni interface, which indicates that Ni atoms dissolve into the solder and react with Sn. So electroplated-Ni is often used as a barrier layer on the PCB.

To further analyze the function of the shear stress-strain behavior on diffusion and IMC growth, the relationship of IMC growth and the square root of time can be investigated under the thermal-shear cycling condition according to Eq 1:

$$\frac{dY}{dt} = K\sqrt{D}t^{-\frac{1}{2}} \quad \text{(Eq 3)}$$

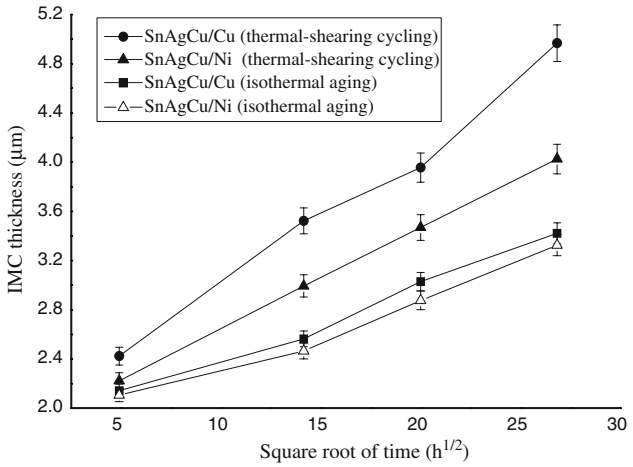

Fig. 5 Comparison of IMCs growth at SnAgCu/Cu and SnAgCu/Ni interfaces under different two conditions

Table 1 Cu atoms diffusion coefficient under the thermal-shearing cycling condition (μm²/s)

Condition	Isothermal aging	Thermal-shearing cycling for Cu substrate	Thermal-shearing cycling for Ni substrate
Diffusion coefficient	1.89×10^{-6}	4.25×10^{-5}	2.25×10^{-5}

$$Y = \int_0^a K\sqrt{D_0}t^{-\frac{1}{2}}dt + \int_a^b K\sqrt{D'}t^{-\frac{1}{2}}dt = y_0 + \sqrt{D_0 t_0 + D' t_1} = y_0 + \left(D_0 t_0 + D' 2N\phi\gamma t_{\text{ramp}}\nu\right)^{\frac{1}{2}} \quad \text{(Eq 4)}$$

where y_0 is the thickness of the IMC after reflow, N is a kinetic constant representing strain-enhanced aging, t_{ramp} is the up or down ramp time during one cycle, ϕ is the ratio of plastic strain to total strain imposed during the ramp, γ is the shear strain rate imposed on the joint and ν is the number of cycles. Dutta et al. (Ref 14) presented the equation of coarsening kinetics of Ag_3Sn particles under isothermal aging and thermal-mechanical cycling (TMC). But the former is suitable for the precipitation and growth of particles in the solder, while the IMC growth at the interface is mainly controlled by the atomic diffusion. So the latter equation may be more appropriate, because it relates the strain rate and IMC thickness.

In order to reduce measurement errors, the fitted trendlines were selected to investigate the relationship between the thickness of IMC and square root of thermal-shear cycling time. The diffusion coefficient D' of Cu under thermal-shear cycling condition is about 10^{-5} μm²/s, which is one-digit growth higher than that under the isothermal aging condition, as shown in Table 1. The results indicate that shear stress-strain is useful to atomic diffusion and IMC growth.

3.3 Ag_3Sn Growth

It is found that Ag_3Sn IMCs, Ag 75.24 at.% and Sn 24.76 at.%, exist in the form of uniform particles or large branches during the initial reflow process and after thermal-shear cycling in the body of solder, as shown in Fig. 2 and 4. It is reported that large branch-like Ag_3Sn structures grow rapidly in liquid phase, during cooling and before the final solidification of solder joints, when the content of Ag is more than 3.5 wt.% in the lead-free solder (Ref 15-17). As verified in this paper, there are planar-type Ag_3Sn IMCs near the interfaces and the particles in the solder after the reflow process. In the shear-cyclic dependent regime, the thickness of Cu_6Sn_5 and $(Cu_xNi_{1-x})_6Sn_5$ IMCs grows remarkably. At the same time, with the IMC thickness growth and Cu and Sn depletion, the numbers of Ag increase at the surface between $(Cu_xNi_{1-x})_6Sn_5$ and Cu_6Sn_5 IMCs and the solder. Therefore, Ag_3Sn IMC is easy to shape and congregate into platelets surrounding the $(Cu_xNi_{1-x})_6Sn_5$ and Cu_6Sn_5 compounds, as in Fig. 2-4.

Furthermore, Ag_3Sn IMC near Cu_6Sn_5 IMC grows faster than that surrounding the $(Cu_xNi_{1-x})_6Sn_5$ IMC because growth rate of Cu_6Sn_5 IMC at Cu substrate is faster than that of $(Cu_xNi_{1-x})_6Sn_5$ IMC and consumes large amounts of Cu and Sn. During the cyclic process, with the thickness of Cu_6Sn_5 and $(Cu_xNi_{1-x})_6Sn_5$ IMC further increasing, Ag-rich phase gathers around the interfaces. It accelerates the planar Ag_3Sn growth, extending at grain boundary and merging together at last. Figure 4(a) shows a typical micrograph of two large Ag_3Sn platelets merging together after 720 cycles at the Cu substrate, which is parallel to the direction of shear stress and it has less effect on the enhancement of the solder strength (Ref 15).

Figure 6 shows the cross-section SEM image of Ag_3Sn IMC in the solder under isothermal aging and thermal-shear cycling conditions. It can be observed that the Ag_3Sn morphology is nearly spherical and hardly changed after isothermal aging and thermal-shear cycling. However, the average Ag_3Sn particles sizes increased under the two conditions, and the particles coarsened more remarkably under thermal-shear cycling than after isothermal aging. It suggested that shear stress increased the crystal lattice distortion, which promoted Ag and Sn diffusion. Because the Ag atom diffusion velocity at relatively lower preservation temperature (25 °C) is much lower than that at relatively higher preservation temperature (125 °C), the Ag_3Sn particles coarsened in the solder and near the two interfaces were enriched mainly by the Ag atoms at 125 °C. The particle sizes have been measured in three different regions to get the average value in the solder and near the interfaces. The relationships between average sizes of Ag_3Sn particles in the solder and cyclic time at 125 °C are presented in Fig. 7. The relationships between Ag_3Sn particle average radius and cyclic time at 125 °C are presented in Fig. 8. It can be proved that the average size of Ag_3Sn increases with increasing cyclic time. The growth rate of particles under thermal-shear cycling is higher than that under isothermal aging, which suggested that crystal lattice distortion generated by shear stress is useful to diffusion and particle growth. The average radius of large platelets of Ag_3Sn IMC near the two interfaces is larger than that in the solder. Therefore, $(Cu_xNi_{1-x})_6Sn_5$ and Cu_6Sn_5 IMCs growth remarkably promotes the development of Ag_3Sn. The larger the thickness of $(Cu_xNi_{1-x})_6Sn_5$ and Cu_6Sn_5 IMCs, the larger will be the thickness of platelets of Ag_3Sn IMC which are harmful to the solder reliability. Therefore, the solder joints during the thermal-shear cycling are more fragile than the joints under isothermal aging.

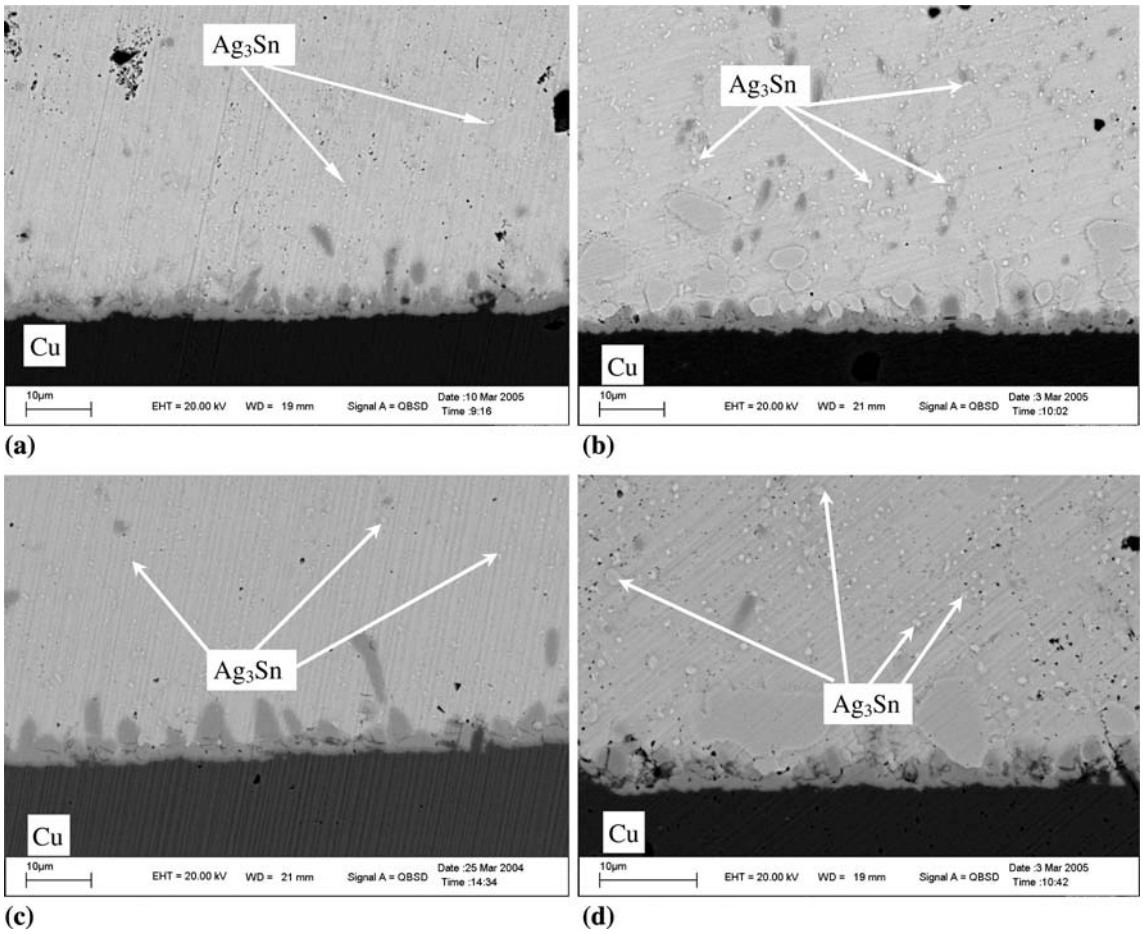

Fig. 6 SEM picture of Ag3Sn IMC in SnAgCu solder under the two conditions after (a) 100 and (b) 360 isothermal aging hours, (c) 200 and (d) 720 thermal-shear cycling cycles

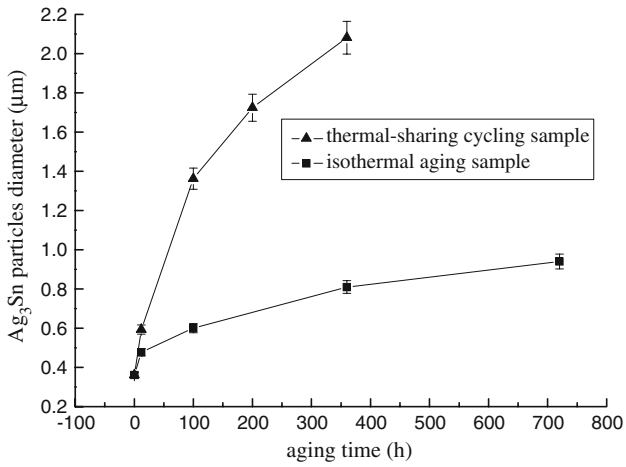

Fig. 7 The relationship between Ag3Sn particles sizes and aging time in the Sn3.5Ag0.5Cu solder alloy under the two conditions

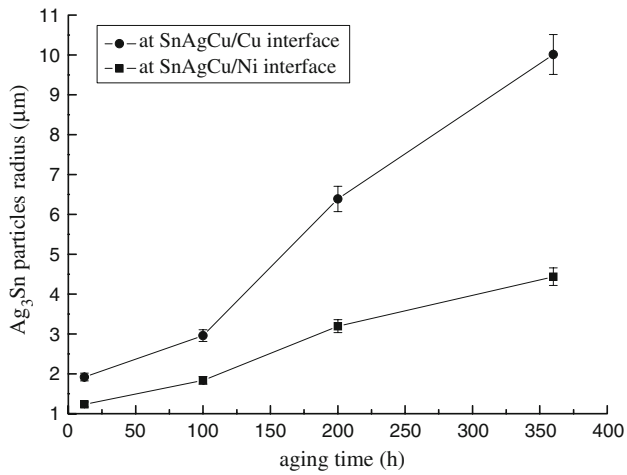

Fig. 8 The relationship between Ag_3Sn particles sizes and aging time at two interfaces

4. Conclusion

1. There are only single Cu_6Sn_5 and $(Cu_xNi_{1-x})_6Sn_5$ IMC layers formed at Sn3.5Ag0.5Cu/Cu and Sn3.5Ag0.5Cu/Ni interfaces after 720 cycles, respectively. The compound morphology changes gradually from scallop-like to planar-like, and planar-like IMC that has lower surface energy to the solid solder is stable in solid state.
2. The IMC formation and growth at Sn3.5Ag0.5Cu/Ni or Cu interfaces are controlled by the dissolution and diffusion of Cu atoms after isothermal aging and thermal-shear cycling. The combined effects of thermal treatment

and shear-stress lead to crystal lattice distortion and promote growth of IMC. The equation of compound growth was given, and the average diffusion coefficient of Cu in IMCs is estimated to be about 10^{-5} $\mu m^2/s$ at the two interfaces under thermal-shear cycling. This value is higher than that under isothermal aging at 125 °C.

3. The Ag_3Sn IMCs formed uniform particles in the solder or large branches near the interfaces after reflow. The particles are easily congregated under thermal-shear cycling. The congregation of the branch-type Ag_3Sn is detrimental to the mechanical properties of the solder joints.

Acknowledgment

This work was supported by the National Natural Science Foundation of China (No. 50371010).

References

1. J.Y. Tsai and C.R. Kao, The Effect of Ni on the Interfacial Reaction Between Sn-Ag Solder and Cu Metallization, *Proceedings of the 4th International Symposium on Electronic Materials and Packaging Conference* (Taiwan, China), IEEE Press, 2002, p 271–276
2. Y.S. Kim, K.S. Kim, and C.W. Hwang, et al., Effect of Composition and Cooling Rate on Microstructure and Tensile Properties of Sn-Zn-Bi Alloys, *J. Alloys Compd.*, 2003, **352**(3), p 237–245
3. X. Ma, F.J. Wang, and Y.Y. Qian, et al., Development of Cu-Sn Intermetallic Compound at Pb-Free Solder/Cu Joint Interface, *Mater. Lett.*, 2003, **57**(22–23), p 3361–3365
4. K.S. Kim, J.M. Yang, C.H. Yu, and I.O. Jung, et al., Analysis on Interfacial Reactions Between Sn-Zn Solders and the Au/Ni Electrolytic-Plated Cu Pad, *J. Alloys Compd.*, 2004, **379**(1/2), p 314–318
5. C.L. Wei and C.R. Kao, Liquid/Solid and Solid/Solid Reactions Between SnAgCu Lead-Free Solders and Ni Surface Finish, *Proceedings of the 4th International Symposium on Electronic Materials and Packaging Conference* (Taiwan, China), IEEE Press, 2002, p 330–334
6. C.M. Chang, P.C. Shi, and K.L. Lin, Interfacial Reaction Between Sn-Ag-Cu, Sn-Ag-Cu-Ni-Ge Lead-Free Solders and Metallic Substrates, *Proceedings of the 4th International Symposium on Electronic Materials and Packaging Conference* (Taiwan, China), IEEE Press, 2002, p 360–366
7. H.L.J. Pang, K.H. Tan, X.Q. Shi, and Z.P. Wang, Microstructure and Intermetallic Growth Effects on Shear and Fatigue Strength of Solder Joints Subjected to Thermal Cycling Aging, *Mater. Sci. Eng. A*, 2001, **307**, p 42–50
8. A. Sharif, Y.C. Chan, M.N. Islam, and M.J. Rizvi, Effect of Indium Addition in Sn-Rich Solder on the Dissolution of Cu Metallization, *J. Alloys Compd.*, 2005, **388**, p 75–82
9. S. Wiese, F. Feustel, and E. Meusel, Characterisation of Constitutive Behaviour of SnAg, SnAgCu and SnPb Solder in Flip Chip Joints, *Sens. Actuators A*, 2002, **99**, p 188–193
10. K.H. Prakash and T. Sritharan, Interface Reaction Between Copper, Molten Tin-Lead Solders, *Acta Mater.*, 2001, **49**, p 2481–2489
11. O. Fouassier, J. Chazelas, and J.F. Silvain, Conception of a Consumable Copper Reaction Zone for a NiTi/SnAgCu, *Compos. Mater. A*, 2002, **33**, p 1391–1395
12. L. Qin, J. Zhao, and L. Wang, et al., Microstructure Evolution in Lead-Free Solder Joints After Wave Soldering and Reflow Soldering, *Electron. Process Technol.*, 2004, **25**(2), p 64–67
13. H.L.J. Pang, T.H. Low, and B.S. Xiong, et al., Thermal Cycling Aging Effects on Sn-Ag-Cu Solder Joint Microstructure, IMC and strength, *Thin Solid Films*, 2004, **462–463**, p 370–375
14. I. Dutta, D. Pan, and R.A. Marks, et al., Effect of Thermo-Mechanically Induced Microstructural Coarsening on the Evolution of Creep Response of SnAg-Based Microelectronic Solders, *Mater. Sci. Eng. A*, 2005, **410–411**(25), p 48–52
15. J. Zhao, Y. Miyashita, and Y. Mutoh, Fatigue Crack Growth Behavior of 96.5Sn-3.5Ag Lead-Free Solder, *Int. J. Fatigue*, 2001, **23**, p 723–731
16. D.W. Henderson, T. Gosselin, and A. Sarkhel, Ag_3Sn Plate Formation in the Solidification of Near Ternary Eutectic Sn-Ag-Cu Alloys, *J. Mater. Res.*, 2002, **17**, p 2775–2778
17. K.S. Kim, S.H. Huh, and K. Suganuma, Effect of Intermetallic Compounds on Properties of Sn-Ag-Cu Lead-Free Soldered Joints, *J. Alloys Compd.*, 2003, **352**, p 226–236